

Observation of parabolic nondiffracting optical fields

Carlos López–Mariscal, Miguel A. Bandres, and Julio C. Gutiérrez–Vega

Photonics and Mathematical Optics Group, Tecnológico de Monterrey, Monterrey, México
64849

juliocesar@itesm.mx

Sabino Chávez–Cerde

Instituto Nacional de Astrofísica Óptica y Electrónica, A. P. 51/216, Puebla, México 72000

Abstract: We report the first experimental observation of parabolic nondiffracting beams, the fourth fundamental family of propagation-invariant optical fields of the Helmholtz equation. We generate the even and odd stationary parabolic beam and with them we are able to produce traveling parabolic beams. It is observed that these fields exhibit a number of unitary in-line vortices that do not interact on propagation. The experimental transverse patterns show an inherent parabolic structure in good agreement with the theoretical predictions. Our results exhibit a transverse energy flow of traveling beams never observed before.

© 2005 Optical Society of America

OCIS codes: (260.1960) Diffraction theory. (350.5500) Propagation.

References and links

1. J. Durnin, "Exact solutions for nondiffracting beams. I The scalar theory," *J. Opt. Soc. Am. A* **4**, 651–654 (1987).
2. J. Durnin, J. J. Micely Jr., and J. H. Eberly, "Diffraction-Free Beams," *Phys. Rev. Lett.* **58**, 1499–1501 (1987).
3. S. Chávez-Cerde, "A new approach to Bessel beams," *J. Mod. Opt.* **46**, 923–942 (1999).
4. J. C. Gutiérrez-Vega, M. D. Iturbe-Castillo, and S. Chávez-Cerde, "Alternative formulation for invariant optical fields: Mathieu beams," *Opt. Lett.* **25**, 1493–1495 (2000).
5. J. C. Gutiérrez-Vega, M. D. Iturbe-Castillo, G. A. Ramírez, E. Tepichín, R. M. Rodríguez-Dagnino, S. Chávez-Cerde, and G.H.C. New, "Experimental demonstration of optical Mathieu beams," *Opt. Commun.* **195**, 35–40 (2001).
6. S. Chávez-Cerde, M. J. Padgett, I. Allison, G. H. C. New, J. C. Gutiérrez-Vega, A. T. O'Neil, I. MacVicar, and J. Courtial, "Holographic generation and orbital angular momentum of high-order Mathieu beams," *J. Opt. B: Quantum Semiclass. Opt.* **4**, S52–S57 (2002).
7. M. A. Bandres, J. C. Gutiérrez-Vega, and S. Chávez-Cerde, "Parabolic nondiffracting optical wave fields," *Opt. Lett.* **29**, 44–46 (2004).
8. J. F. Nye and M. V. Berry, "Dislocations in wave trains," *Proc. R. Soc. Lond. A* **336**, 165–190 (1974).
9. D. L. Feder, A. A. Svidzinsky, A. L. Fetter and C. W. Clark, "Anomalous Modes Drive Vortex Dynamics in Confined Bose-Einstein Condensates," *Phys. Rev. Lett.* **86**, 564–567 (2001).
10. I. S. Aranson, A. R. Bishop, I. Daruka and V. M. Vinokur, "Ginzburg-Landau Theory of Spiral Surface Growth," *Phys. Rev. Lett.* **80**, 1770–1773 (1998).
11. C. O. Weiss, M. Vaupel, K. Staliunas, G. Sleky and V. B. Taranenko, "Solitons and vortices in lasers," *Appl. Phys. B* **68**, 151–168 (1999).
12. G. Indebetouw, "Nondiffracting optical fields: some remarks on their analysis and synthesis," *J. Opt. Soc. Am. A* **6**, 150–152 (1989).
13. H. I. Bjelkhagen, *Silver-halide recording materials* (Springer, Berlin, 1993) Ch. 5.
14. K. Volke-Sepúlveda, V. Garcés-Chávez, S. Chávez-Cerde, J. Arlt, and K. Dholakia, "Orbital angular momentum of a high-order Bessel light beam," *J. Opt. B: Quantum Semiclass. Opt.* **4**, S82–S89 (2002).

15. V. Garcés-Chávez, D. McGloin, H. Melville, W. Sibbett, and K. Dholakia, "Simultaneous micromanipulation in multiple planes using a self-reconstructing light beam," *Nature* **419**, 145–147 (2002).
16. K. T. Gahagan and G. A. Swartzlander, Jr., "Optical vortex trapping of particless," *Opt. Lett.* **21**, 827–829 (1996).
17. M. Erdélyi, Z. L. Horváth, G. Szabó, S. Bor, F. K. Tittel, J. R. Cavallaro, and M. C. Smayling, "Generation of diffraction-free beams for applications in optical microlithography," *J. Vac. Sci. Technol. B* **15**, 287–292 (1997).
18. J. Y. Lu and S. He, "Optical X wave communications," *Opt. Commun.* **161**, 187–192 (1999).

Propagation-invariant optical fields (PIOFs) are of interest since, ideally, their transverse intensity distribution remains unchanged upon propagation. Because of this feature, their spatial evolution has been extensively studied and numerous applications have been proposed. It is known that plane waves, Bessel beams [1, 2, 3] and Mathieu beams [4, 5, 6] correspond to three different fundamental families of PIOFs, each associated to a corresponding solution of the Helmholtz equation (HE) in Cartesian, circular cylindrical, and elliptic cylindrical coordinates, respectively. Recently, the existence of parabolic beams (PBs), the fourth and last fundamental family of PIOFs, was demonstrated theoretically [7]. Contrary to Bessel and Mathieu beams, even for low order, PBs can have a large number of vortices of unitary charge and rotating in the same direction, all of them are aligned along the symmetry axis and whose phase gradient between any two vortices is zero. This makes them propagate without interaction, that is contrary to other observed vortices embedded in arbitrary background fields reported in the literature [8, 9, 10, 11].

In this paper, we present the first experimental observation of nondiffracting PBs. We generate finite versions of stationary zero-order and high-order, even and odd PBs, and analyze their behavior upon propagation. A suitable superposition of these high-order stationary beams allow us to build a new kind of traveling parabolic beams whose phase travels following con-focal parabolic trajectories [7]. On free space propagation the transverse energy flow presents a very interesting parabolic twisting behavior never observed before in wavefields, to the best of our knowledge. It is observed that PBs exhibit a number of unitary in-line vortices that do not interact on propagation.

Fundamental PIOFs of the HE are written as $U(\mathbf{r}) = \exp(-ik_z z) u(\mathbf{r}_t)$, where \mathbf{r}_t denotes the transverse coordinates. The transverse field $u(\mathbf{r}_t)$ can be expressed in terms of the Whittaker integral

$$u(\mathbf{r}_t) = \int_{-\pi}^{\pi} A(\varphi) \exp[-ik_t(x \cos \varphi + y \sin \varphi)] d\varphi, \quad (1)$$

where $A(\varphi)$ is the angular spectrum of the PIOF and the transverse and longitudinal wave vector components satisfy the relation $k^2 = k_t^2 + k_z^2$. By defining the parabolic cylindrical coordinates $\mathbf{r}_t = (\xi, \eta)$ as $x = (\eta^2 - \xi^2)/2$, $y = \xi\eta$, where $\xi \in [0, \infty)$, and $\eta \in (-\infty, \infty)$, the transverse field distributions of the even and odd stationary PBs are found to be [7]

$$u_e(\mathbf{r}_t; a) = \frac{|\Gamma_1|^2}{\pi\sqrt{2}} P_e(\sigma\xi; a) P_e(\sigma\eta; -a), \quad (2)$$

$$u_o(\mathbf{r}_t; a) = \frac{2|\Gamma_3|^2}{\pi\sqrt{2}} P_o(\sigma\xi; a) P_o(\sigma\eta; -a), \quad (3)$$

where $\sigma \equiv (2k_t)^{1/2}$, $\Gamma_1 \equiv \Gamma(1/4 + ia/2)$, and $\Gamma_3 \equiv \Gamma(3/4 + ia/2)$. Having failed to find a better term, we will term the continuous parameter $a \in (-\infty, \infty)$ the order of the beam. Here, $P_e(v; a)$ and $P_o(v; a)$ are the even and odd real solutions of the parabolic cylinder differential equation

$(d^2/dx^2 + x^2/4 - a)P(x;a) = 0$. Angular spectra for the PBs in Eqs. (2) and (3) are given by

$$A_e(\varphi;a) = \frac{1}{2(\pi|\sin\varphi|)^{1/2}} \exp\left(ia \ln \left| \tan \frac{\varphi}{2} \right| \right), \quad (4)$$

$$A_o(\varphi;a) = \frac{1}{i} \begin{cases} -A_e(\varphi;a), & \varphi \in (-\pi, 0) \\ A_e(\varphi;a), & \varphi \in (0, \pi) \end{cases}, \quad (5)$$

respectively. Transverse theoretical patterns of stationary PBs are shown in Ref. [7] for several values of the parameter a .

High-order Bessel beams and Mathieu beams [6] have a phase that rotates circularly and elliptically about the propagation axis, respectively. Following the same approach, using a proper linear combination of the parabolic stationary solutions Eqs. (2) and (3) we have constructed the traveling PBs

$$TU^\pm(\mathbf{r};a) = [u_e(\mathbf{r}_t;a) \pm iu_o(\mathbf{r}_t;a)] \exp(-ik_z z), \quad (6)$$

whose overall phase now travels around the semiplane ($x \geq 0, z$) for $a > 0$. When observed at fixed transverse planes the phase seems to follow confocal parabolic trajectories. The sign in Eq. (6) defines the traveling direction. For $a > 0$, the transverse intensity pattern consists of well-defined nondiffracting parabolic fringes with a dark parabolic region around the positive x axis [7]. From Eqs. (4) and (5), the angular spectra of the traveling PBs are given by $A^\pm(\varphi;a) = A_e(\varphi;a) \pm iA_o(\varphi;a)$.

Our approach for the generation of PIOFs aimed at a reliable technique for consistently producing their angular spectra. Subsequent Fourier transformation by a corrected lens of radius R and focal distance f resulted in the desired field distribution. Evidently, the aperture of the lens imposes a boundary for the spatial extent of the beam while ideally, its propagation is strictly invariant only if the beam would be of infinite transverse extension.

In the particular case of the zero-order PBs, the angular spectrum in Eq. (4) is real and positive for all values of φ . Based on the McCutchen theorem [12], one can thus construct the corresponding angular spectrum by means of a thin annular slit modulated by $A_e(\varphi;a=0)$ in a variation of the setup originally used by Durnin *et al.* [1, 2] for generating Bessel beams, and more recently used by Gutiérrez-Vega *et al.* [5] for Mathieu beams. We used an annular slit with radius $r_0 = 0.5$ mm and thickness $\Delta r_0 = 25$ μ m. The angular modulation was accounted for by a properly exposed photographic film with the angular function $A_e(\varphi;a=0)$. In this case, additional spatial bounds are determined by the finite thickness of the annular slit. For the odd beam a tilted glass plate, introduced in the half-region $\varphi \in (-\pi, 0)$, makes up for the required relative phase-shift of π radians. A larger ring ($r_0 = 1.0$ mm, $\Delta r_0 = 47$ μ m) was used in this case to make more accurate the positioning placing of the glass plate. The resulting diffractive optical element is then illuminated by a plane wave from a He-Ne 15 mW laser source ($\lambda = 632.8$ nm). In Fig. 1, the experimental transverse intensity profiles of the even and odd zero-order PBs are observed at different distances along the propagation axis. The resulting patterns clearly exhibit well defined parabolic nodal lines, and are symmetrical along the x and y axes. As expected, the odd mode vanishes along the x axis. Note that within the sampled distance, the beam is practically invariant and changes in the intensity distribution are only minor.

For high-order stationary and traveling PBs, the phase of the spectrum in Eqs. (4) and (5) becomes a rapidly varying function. Attempting to generate the spectrum by means of the same approach used for zero-order beams showed to be impractical. Instead, we made use of blazed phase computer-generated holograms (CGH). The holograms were photoreduced and subsequently bleached to attain a higher diffraction efficiency [6, 13]. The corresponding stationary transverse intensity profiles are shown in Fig. 2 for the even and odd beams with $a = 4$. Notice that the value of a is not restricted to take integer values[7]. Here, further spatial limits are

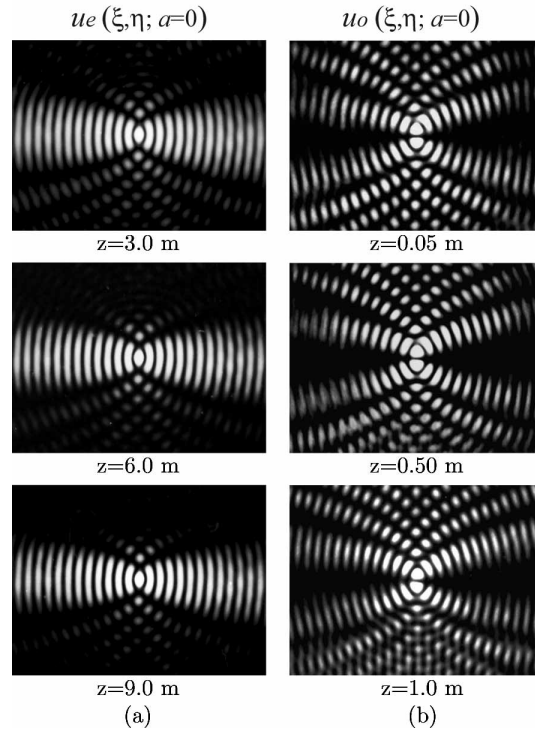


Fig. 1. Experimental transverse intensity profiles of the (a) even and (b) odd PBs for $a = 0$. For the even beam $f = 30$ cm and $R = 4.5$ cm, whereas for the odd beam $f = 15$ cm, $R = 2.5$ cm and z is the distance from the lens.

imposed by the size of the CGH, however, the profiles remain nearly unchanged as the beam propagates. The similarity with the theoretical patterns is remarkable.

Traveling PBs can be generated with a suitable superposition of stationary PBs. The propagating behavior of the traveling fields is expected to be different from that of the stationary fields. Due to its phase distribution, transverse energy flow must occur along parabolic trajectories. As with the other families of PIOFs these PBs remain invariant within a conical volume for the setup used. In our experiment, the spatial extent of the fields is limited by the physical boundaries of the CGH and the finite aperture of the lens. Such behavior for the transverse energy flow of the traveling PB $TU^-(\eta, \xi; a = 4)$ is clearly observed in the photographic sequence shown in Fig. 3(a). Note that the energy flows within the parabolic nodal lines and around the positive x axis. The light intensity moves away from the region originally occupied by the beam, this is well observed at the upper section ($y > 0$) the corresponding parabolae have apparently vanished. In the far-field, the intensity pattern of the $TU^-(\eta, \xi; a = 4)$ beam tends to acquire the shape of its angular spectrum, namely a semi-circular ring whose amplitude is proportional to $|A_e(\varphi; a)|^2$ for $\varphi \in (-\pi, 0)$ and vanishes elsewhere.

In order to verify the dynamic behavior of the traveling PBs, the three-dimensional spatial evolution of the field was numerically calculated by solving the Helmholtz equation and using the corresponding initial condition. We show in Fig. 3(b) the simulated transverse intensity distributions. The results shown in Fig. 3 are of particular relevance since they clearly illustrate the behavior of the transverse energy flow occurring in the traveling PBs. Even though this effect also takes place in high-order Bessel and traveling Mathieu beams for which their nodal lines are closed, in the case of PBs these never close making this effect more significant.

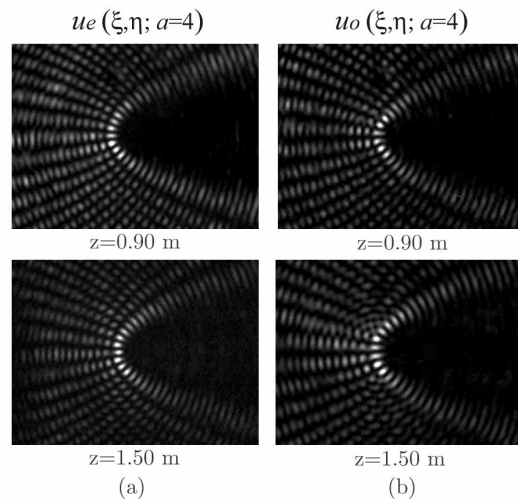


Fig. 2. Experimental transverse intensity profiles of the even (a) and odd (b) high-order PBs for $a = 4.0$ at different distances along the propagation axis.

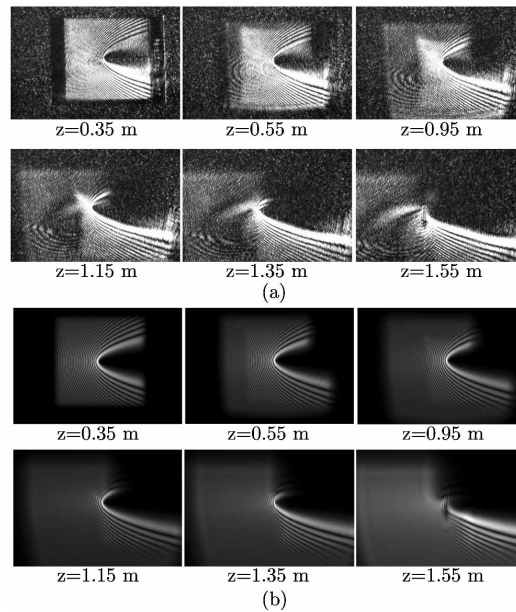
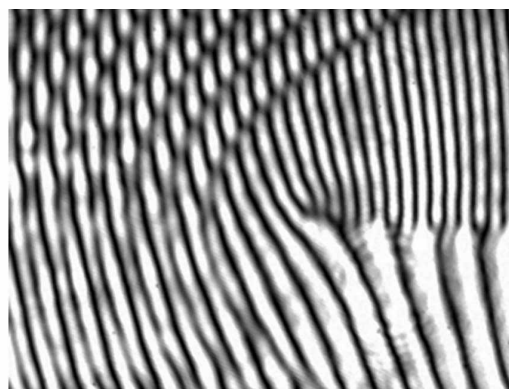


Fig. 3. a) Photographic sequence of the propagation of a bounded traveling PB $TU^-(\eta, \xi; a = 4)$. (b) Computer simulated propagation.

The phase structure of the PBs can be studied by interfering it with a plane wave. For a traveling PB with $a > 0$ the principal branch of vortices occurs along the positive x axis ($\xi = 0$) at points $x_j = \eta_j^2/2$, where $j = 1, 2, \dots, \infty$, and η_j are the zeros of the even parabolic function $P_e(\sigma\eta; -a)$ in the interval $\eta \in [0, \infty)$. The phase of an ideal PB then has an infinite number of in-line vortices lying along the positive x axis, each with unitary topological charge. The interferogram between the initial traveling beam in Fig. 3 and a plane wave is shown in Fig. 4. As predicted by the zeros of the function $P_e(\sigma\eta; -a)$, after the first two vortices, the spacing between phase dislocations becomes nearly constant. Increasing the value of a has the effect of displacing the locus of the first vortex towards larger values of x , and increasing the spacing between adjacent vortices.

Since the electromagnetic fields presented here belong to the families of PIOFs their vortices must remain in their position as long as the condition for invariance is fulfilled [3]. In other words, the vortices have zero phase gradient between them that results in neither attraction nor repulsion between each other. A question that arises from looking at the vortex structure and the overall phase, is about what kind of relation links optical and mechanical angular momentum of these beams? The answer to this question is beyond the scope of the present paper, however the results of such study will be presented elsewhere.

In conclusion, we have successfully generated a new family of propagation invariant optical fields. They are the parabolic beams that constitute the fourth and last family of fundamental PIOFs of the Helmholtz equation. In particular, we analyzed the evolution of traveling PBs whose transverse energy flow follows confocal parabolic helices. These fields have a large number of inline co-rotating vortices, its number depending either on the order mode or on the extent of our initial condition, i.e., the extent of the input aperture. Similar to Bessel beams [14, 15], the PBs presented here can be applied to optical tweezers and atom traps, to study the transfer of angular momentum to microparticles or atoms [16], in lithography [17], and optical communications [18].



$z=0.35$ m

Fig. 4. Interference pattern between the generated traveling beam $TU^-(\eta, \xi; a = 4)$ and a reference plane wave. A number of in-line vortices lying along the positive x axis are observed.

Acknowledgments

This work was partially supported by CONACyT México grant 42808 and by the Tecnológico de Monterrey grant CAT-007. S.Chávez-Cerda acknowledges support by Tecnológico de Monterrey.